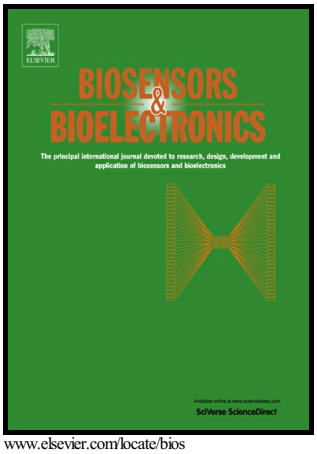

www.elsevier.com/locate/bios

Direct Label-free Protein Detection in High Ionic Strength Solution and Human Plasma Using Dual-Gate Nanoribbon-based Ion-Sensitive Field-Effect Transistor Biosensor

Shenhui Ma, Xin Li, Yi-Kuen Lee, Anping Zhang

PII: S0956-5663(18)30421-4
DOI: https://doi.org/10.1016/j.bios.2018.05.061
Reference: BIOS10519

To appear in: *Biosensors and Bioelectronic*

Received date: 13 April 2018
Revised date: 28 May 2018
Accepted date: 31 May 2018

Cite this article as: Shenhui Ma, Xin Li, Yi-Kuen Lee and Anping Zhang, Direct Label-free Protein Detection in High Ionic Strength Solution and Human Plasma Using Dual-Gate Nanoribbon-based Ion-Sensitive Field-Effect Transistor Biosensor, *Biosensors and Bioelectronic,* https://doi.org/10.1016/j.bios.2018.05.061

Direct Label-free Protein Detection in High Ionic Strength Solution and Human Plasma Using Dual-Gate Nanoribbon-based Ion-Sensitive Field-Effect Transistor Biosensor

Shenhui Ma[1,2], Xin Li[1,3*], Yi-Kuen Lee[2], Anping Zhang[4*]

[1]School of Microelectronics, Xi'an Jiaotong University, Xi'an, Shaanxi 710049, China

[2]Department of Mechanical and Aerospace Engineering, The Hong Kong University of Science and Technology, Hong Kong SAR, China

[3]Guangdong Shunde Xi'an Jiaotong University Academy, Foshan, Guangdong 528300, China

[4]State Key Laboratory of Electrical Insulation and Power Equipment, Xi'an Jiaotong University, Xi'an, Shaanxi 710049, China

lx@mail.xjtu.edu.cn

anpzhang@xjtu.edu.cn

[*]Corresponding author. Tel.: +862982663343

[*]Corresponding author. Tel.: +862982665363

Abstract

We report on direct label-free protein detection in high ionic strength solution and human plasma by a dual-gate nanoribbon-based ion-sensitive field-effect transistor (NR-ISFET) biosensor system with excellent sensitivity and specificity in both solution-gate (SG) and dual-gate (DG) modes. Compared with previously reported results, the NR-ISFET biosensor enables selective prostate specific antigen (PSA) detection based on antibody-antigen binding in broader detection range with lower LOD. For the first time, real-time specific detection of PSA of 10 pM to 1 μM in 100 mM phosphate buffer (PB) was demonstrated by conductance measurements using the polyethylene glycol (PEG)-modified NR-ISFET biosensors in DG mode with the back-gate bias (V_{BG}) of 20 V. Due to larger maximum transconductance value resulting from the modulation of NR-ISFET channel by the back gate in DG mode, the detection range can be broadened with larger linear detection region (100 pM to 100 nM) and lower limit of detection (LOD, 10 pM) as compared to those in SG mode. Moreover, the influence of different back-gate bias from V_{BG} = 5 V to V_{BG} = 25 V on the biosensor performance has been investigated. Furthermore, direct PSA detection of 100 pM to 1 μM in human plasma was demonstrated by using the PEG-modified NR-ISFET in DG mode, enabling direct detection of protein in human blood for clinical applications since the LOD of 100 pM PSA can meet the clinical requirements.

Keywords: DUAL-GATE ISFET BIOSENSOR, LABEL-FREE, REAL-TIME PROTEIN DETECTION, BACK GATE, DEBYE SCREENING LENGTH, HUMAN PLASMA

1. Introduction

Ion-sensitive field-effect transistor (ISFET) was first proposed in the 1970s as a device for neurophysiological monitoring (Bergveld, 1972, 2003; Toumazou et al., 2014), and then commercialized as pH sensor in 1980s (Esashi, 1975; Matsuo and Esashi, 1981). Later, ISFET has been customized to sense various analytes other than pH, opening up a wide range of applications in life sciences. ISFET is electronically identical to a metal-oxide-semiconductor field-effect transistor (MOSFET) and can still be regarded as an electronic device, with one additional feature, i.e., the possibility to chemically modify the threshold voltage via the surface potential at the electrolyte/sensing layer interface (Bergveld, 2003). As for protein detection, the widely used methods include the enzyme-linked immunosorbent assay (ELISA, Ambrosi et al., 2009), fluorescence-based and chemiluminescence-based methods (Xu et al., 2011), surface plasmon resonance (SPR, Zeng et al., 2014) etc., which are usually restricted by the time-consuming labeling steps, sophisticated and expensive optical instrumentation or low sensitivity. Compared with these conventional methods, ISFET-based biosensors have enabled the direct, rapid, label-free and low-cost protein detection with high sensitivity and selectivity. One of the limitations in the ISFET-based protein detection is that the change in surface potential induced by protein association/dissociation are often small (Nair and Alam, 2008; Zeimpekis et al., 2016) so it is more difficult to detect current changes in the semiconductor than those resulting from ion association/dissociation (Zeimpekis et al., 2016). To overcome this limitation, nanoribbon/nanowire-based ISFET (NR/NW-ISFET) devices have been employed for real-time label-free detection of a wide range of biological species with high sensitivity due to larger surface to-volume ratio compared to conventional ISFET (Jang and Cho, 2011; Tarasov et al., 2011), including pH detection (Chen et al., 2011; Knopfmacher et al., 2010; Peretz-Soroka et al., 2013; Sun et al., 2016), DNA detection (Bunimovich et al., 2006; Gao et al., 2012; Hao et al., 2014; Ma et al., 2018; Xie et al., 2012; Zhang et al., 2008), protein detection (Elfström et al., 2008; Hakim et al., 2012; Hu et al., 2016; Kumar M et al., 2011; Selvanayagam et al., 2002; Stern et al., 2007; Yacoub-George et al., 1996; Yu et al., 2013), etc. However, these sensing measurements were usually conducted in the non-physiological solutions in low ionic strength due to the effect of Debye-screening length (Stern et al., 2007). In physiological solutions, the Debye length is only about 0.7 nm, in which any charge from a bound molecule beyond this distance will be effectively screened by the solutions (Hu et al., 2016).

To date, several methods have been demonstrated to overcome this limitation. In general, indirect methods have been reported which included a desalting step to enable subsequent protein detection in low ionic strength solutions (Duan et al., 2012; Hakim et al., 2012; Stern et al., 2010; Zheng et al., 2005), which were not real-time measurements. Other direct methods have also been demonstrated including the use of short molecular receptors to reduce the distance between the FET surface and the analyte to be detected (Elnathan et al., 2012; Maehashi et al., 2007). More recently, a direct strategy has been proposed to overcome this limitation by using biopermeable PEG layer for modification of a silicon NW-ISFET biosensor surface to increase the effective

Debye screening length, by which the effective dielectric constant at sensor surface is reduced compared with aqueous solution. This method is more promising for real-time direct protein detection in physiological solution and applicable to both in vitro and in vivo sensing (Gao et al., 2015, 2016) as compared to other methods.

Here we have applied a similar strategy on a dual-gate NR-ISFET biosensor for PSA detection in high ionic strength solutions and human plasma. The dual-gate structure enables the modulation of NR-ISFET's sensitivity by the back gate. And the incorporation of specific receptors based on the strategy mentioned above can realize the selective PSA detection. The top-down fabrication technology of NR-ISFETs is simpler with good repeatability and low cost for the mass manufacture of biosensors as compared to bottom-up nanowire fabrication techniques (Hu et al., 2016). Direct label-free detection of PSA in a broad concentration range has been demonstrated with excellent sensitivity and specificity. The NR-ISFET chip was characterized by electrical characterization first. Then real-time conductance measurements of the NR-ISFET biosensor system were conducted with the delivery of PSA in 100 mM PB in SG and DG modes. Different back-gate voltages were applied in the sensing measurements, in which the effect of back gate on the NR-ISFET biosensor performance was investigated. Furthermore, human plasma samples spiked with PSA of different concentrations were directly detected by the NR-ISFET biosensor in SG and DG modes. This method has great potential for direct quantification and detection of biomarker proteins in human blood.

2. Material and methods

2.1 Device fabrication

NR-ISFET devices (Fig. 1(a)) were fabricated on a 2 cm × 2 cm chip using processes similar to these described previously (Shalev et al., 2009, 2012), but with additional anisotropic etching. The silicon-on-insulator (SOI) wafer with a buried oxide (BOX) layer of 375 nm in thickness was used. A 200-nm thick p-type SOI layer was oxidized to reduce to 80 nm by thermal oxidation. Then a layer of photoresist (PR1-4000A, Futurrex, Inc.) was coated on top of the SiO_2. Photolithography (MJB4, SUSS MicroTecn AG) was used to pattern the top oxide masking layer. The Si NRs were fabricated using dry etching of the thinned Si layer (ICP180, Oxford Instruments PLC), followed by ion implantation (P^+) to the drain and source regions to form ohmic contacts. Then anisotropic etching via potassium hydroxide (KOH) and further dry oxidation were conducted to reduce NRs' lateral dimensions. Titanium (Ti, 50 nm) and gold (Au, 150 nm) were subsequently deposited by e-beam evaporation (Ohmiker-50BR, Cello Technology Co., Ltd.) and patterned by lift-off process for metal contacts. A 2-μm thick SU-8 passivation layer (GM 1040, Gersteltec Sarl. Inc.) was coated and patterned as electrical isolation of the contact areas. Additionally, another Au layer (200nm) was deposited onto the gate region before the SU-8 coating for the NR-ISFET used for electrical characterization. The photograph of fabricated chip and scanning electron microscope (SEM, SU-8010, Hitachi, Ltd.) image of NR-ISFETs are shown in Fig. 1(f) and (g). The fabrication process described above is illustrated in Fig. S1. The SEM image of the NR-ISFET's channel after the anisotropic etching of Si NR via KOH and top oxide removal is shown in Fig. S2.

Microchannels (2 mm × 4 mm × 10 μm) were fabricated by mixing polydimethylsiloxane (PDMS) base and

curing agent (10:1, SYLGARD 184 Silicone Elastomer), degassing, silanization treatment of SU-8 (10 μm, GM 1040, Gersteltec Sarl. Inc.) patterned Si wafer by trimethylchlorosilane (TMCS, Sigma-Aldrich Co.), followed by pouring the PDMS mixture onto it, degassing and incubation at 50 °C for 4 h. Polytetrafluoroethylene (PTFE) tubes were used to connect the microchannels to a syringe pump (PhD2000, Harvard Apparatus) for sample delivery.

2.2 Device functionalization

The functionalization process similar to (Gao et al., 2015; Patolsky et al., 2006) was carried out as follows. The fabricated NR-ISFET chips were cleaned in UV/ozone (20 min, No. 42-220, Jelight Company Inc.) and clamped with the PDMS layer patterned with microchannels by two polymethylmethacrylate (PMMA) covers. The silane/ethanol solution was prepared by diluting 1% 3-(trimethoxysilyl)propyl aldehyde (90%, United Chemical Technologies Inc.) in the mixture of 95% ethanol and 5% DI water. The prepared silane/ethanol solution was introduced into the microchannels through the inlet tubing and reacted with the precleaned NR-ISFET chips for 1 h at room temperature, after which the microchannels were rinsed with ethanol for 1 min. Then the sensor chip was modified with silane-PEG (2 h, mPEG-Silane, MW 10k, No. PSB-2016, Creative PEGWorks), anti-PSA antibody receptor (3 h, 1mM in 10 mM PB, pH 8.4, Sigma-Aldrich Co.) and ethanolamine (2 h, 100 mM in 10 mM PB, pH 8.4, Sigma-Aldrich Co.) through the microchannels, respectively. Finally, the sensor surface was rinsed by a continuous flow of 10 mM PB (pH 8.4) through the microchannels for 10 min to wash away the excess reagents.

2.3 Sensing measurements

Before the sensing measurements, the electrical characterization of NR-ISFET chip was carried out by the semiconductor parameter analyzer (Keithley 4200-SCS) using a probe station (S-1160, Signatone Co.). For measurements of transfer characteristics of the NR-ISFETs, the drain-source current (I_{DS}) versus gate-source voltage (V_{GS}) was measured with the drain-source voltage V_{DS} = 2 V. In the sensing measurements, the NR-ISFET chip and PDMS-based microchannels were clamped by two removable polymethyl methacrylate (PMMA) lids, which enabled the sample delivery through inlet and outlet of the microchannels (Fig. 1(h)). The NR-ISFET biosensor system consisted of the NR-ISFET device (Fig. 1(a)) connected to a current preamplifier (DL1211, DL Instruments, Inc.) (Fig. 1(c)) and a lock-in amplifier (SR830, Stanford Research, Inc.) (Fig. 1(b)). The conductance of NR-ISFET ($C = \mathrm{d}I_{DS}/\mathrm{d}V_{DS}$) was measured by use of the lock-in technique, where V_{DS} was modulated at 79 Hz with a 30 mV amplitude while V_{DS}(dc) was set to 0 V (Patolsky et al., 2006; Zheng et al., 2005). The Ag/AgCl reference electrode (V_{RE} = 0 V, Fig. 1(e)) was inserted into the microchannel through an opening to stabilize the solution potential. PSA (Sigma-Aldrich Co.) was used without further purification and directly diluted in different ionic strength PB solutions (pH = 7.4) before the sensing measurements. During the sensing measurements, PB, PSA/PB, human plasma or PSA/human plasma solution was drawn to the microchannel using PTFE tubing attached to the inlet by a syringe pump at a flow rate of 0.3 mL/h, and real-time conductance data was recorded in computer using Labview software (National Instruments Co.).

3. Results and discussion

3.1 Electrical characterization

The electrical characterization of NR-ISFET devices with gold on the gate region of different channel widths (W = 3, 5, 50 μm) was conducted first. The transfer characteristics similar to those of typical MOSFETs have been illustrated in our previous results (Ma et al., 2018), which provide a reliable indicator for subsequent good sensor performance. The threshold voltages of three types of devices are all about 1.80 V. Furthermore, in order to investigate the effects of the back gate, drain-source current (I_{DS}) as a function of back-gate bias (V_{BG}) for three types of NR-ISFET devices was also measured, and the results have also been shown in our previous work (Ma et al., 2018). The drain-source current increased when the back-gate voltage increased from -20 V to 30 V, which indicates that the channel of NR-ISFET can be effectively modulated by the back gate. The back-gate biases are set to 20V in the following experiment to achieve the highest sensitivity in DG mode because the transconductance ($g_m = \mathrm{d}I_{DS}/\mathrm{d}I_{BG}$) can reach the maximum value at about V_{BG} = 20 V.

3.2 PSA detection in high ionic solutions

Initial PSA detection measurements of fixed concentration (100 nM) were carried out with the PEG-modified NR-ISFET devices in PB (pH = 7.4) as a function of solution ionic strength (Fig. 2). PSA/PB solution was delivered at t = 250 s, then after response time of about 200 s a sharp decrease in conductance was observed and the signal became stable after around 20–30 s. The protein solution was switched to PB solution at t = 960 s, and the response signal began to recover to the initial state after about 250 s. The specific binding of the charged PSA to the anti-PSA antibody was detected by the NR-ISFET's surface which induced the conductance variation between the source and drain terminals of NR-ISFET. The decrease in conductance of n-type NR-ISFET was consistent with binding of the negatively charged molecules because the pH of PB solutions (pH 7.4) in the measurement were higher than the isoelectric point of PSA (pI 6.8, Hayes and Barry, 2014). The results in Fig. 2 reveals that the conductance change of PEG-modified NR-ISFET biosensor due to antibody-antigen interaction decreases gradually with increasing PB concentration. The conductance variation in 100 mM PB (ΔC = 0.4 mS) is significant for sensing since the Debye length of 100 mM PB (~0.67 nm) is comparable to physiological solutions. Moreover, conductance change of about 0.35 mS in 150 mM PB can still be detected, where the Debye length is only about 0.54 nm (Gao et al., 2015). Furthermore, bovine serum albumin (BSA, 100 μM)/PB solution (100 mM) was also delivered to the PEG-modified NR-ISFET devices and the response data was shown in Fig. 2. It indicates that the conductance variation for BSA was nearly undetectable, which proves that the NR-ISFET biosensor has achieved good selectivity. Therefore, the results indicate that the modification by silane-PEG, aldehyde-silane and anti-PSA antibody to the NR-ISFET surface was successfully conducted and it can increase the effective screening length in the region adjacent to the device surface, enabling the possibility of specific protein detection in physiological solutions and human plasma.

Then real-time conductance measurements of the PEG-modified NR-ISFET in 100 mM PB with the delivery of PSA solutions of different concentrations in SG mode was conducted (Fig. 3(a)). The PSA concentrations of 1 nM to 1 μM in PB solution were delivered at t = 250 s. After a response time of about 180 s,

the conductance decreased gradually and became stable after around 80–100 s. Here, the measurement process (0–1500 s) can be divided into four periods of time: Region I was from t = 0 s to t = 250 s, which was the time period from the beginning of data record till the delivery of PSA/PB solution; Region II was from t = 250 s to the moment when conductance became stable after introducing the PSA/PB solution (about t = 510–530 s); Region III was from t = 510–530 s to t = 960 s when the sample delivery switched from the protein to PB solution; and Region IV was from t = 960 s to t = 1500 s, which included the antigen-antibody dissociation process (marked in Fig. 3(a)). Therefore, the conductance variation (ΔC) can be calculated as the difference between the average conductance values in Region I and Region III. The conductance variation (0.0772 ± 0.0081 mS to 1.4923 ± 0.1252 mS) for various PSA concentrations (1 nM to 1 μM) was extracted and shown in Fig. 3(b). The sensing response increased with increasing PSA concentration and became saturated when PSA concentration reached 1 μM. From the log-scale curve (the inset of Fig. 3(b)), it reveals that the linear detection region of 10 nM to 100 nM of PSA in SG mode can be achieved in high ionic strength solution. Since the Langmuir adsorption isotherm provides a direct method to quantify an adsorption process, the fitting of Langmuir model to protein adsorption isotherm data is often made to obtain thermodynamic properties, such as the equilibrium constant (Latour, 2015; Tarasov et al., 2015). Therefore, here we also utilize Langmuir model to fit the ΔC–C_{PSA} data as shown below (the fitting curve is depicted in Fig. 3(b)) [39]:

$$\Delta C = \Delta C_{\max} \cdot \frac{k \cdot C_{\mathrm{PSA}}}{k \cdot C_{\mathrm{PSA}} + 1}\ , \tag{1}$$

where ΔC is the change in conductance with $\Delta C_{\max}$ as the saturation value, C_{PSA} is the PSA concentration, and k represents the equilibrium constant during antibody-antigen interaction. The fittings based on Langmuir adsorption isotherm with high coefficient of determination describing how well the regression line approximates the real data points (R^2 = 0.9848) can be achieved, and the fitted equilibrium constant is k = 3.06×10^7 M^{-1} in SG mode. Similar as SG mode, the results of conductance measurements of PEG-modified NR-ISFET in DG mode (V_{BG} = 20 V) are shown in Fig. 3(c). Four periods of time were also defined through the measurement process, and conductance variation induced by the antibody-antigen binding was extracted. As illustrated in Fig. 3(d), in DG mode the conductance variation (0.1834 ± 0.0022 mS to 3.0833 ± 0.2569 mS) as a function of PSA concentration (10 pM to 1 μM) can also be fitted by Langmuir model with high goodness of fit (R^2 = 0.9682) and k = 1.67×10^8 M^{-1}. And the linear detection region of 100 pM to 100 nM of PSA was achieved in DG mode as shown in the log-scale calibration curve (inset of Fig. 3(b)). The equilibrium constants in SG and DG modes both agree well with the reported results for protein adsorption (Latour, 2015; Tarasov et al., 2015). Compared with SG mode, LOD can be reduced from 1 nM to 10 pM in DG mode. The detection based on specific antigen-antibody interaction has broader concentration range and lower LOD as compared to the results reported previously (Gao et al., 2015). The results indicate that the sensor response can be enhanced in terms of signal intensity, sensitivity and LOD if the back-gate bias is applied. With the addition of back-gate bias, the conducting channel is shifted from the surface to the bulk volume of the channel. In this way, scattering will be reduced as compared to that at the interface between the channel and the gate oxide, therefore resulting in higher mobility (Pud et al., 2014). This modulation of the NR-ISFET's channel by the back gate results in

larger maximum transconductance value ($g_{m,max}$) of the NR-ISFET. We hypothesize that with larger $g_{m,max}$ of NR-ISFET, proteins could be detected in higher ionic strength solution (smaller Debye screening length). Therefore, in DG mode, the improved $g_{m,max}$ leads to the expansion of detection range and enhancement of sensitivity if the Debye screening length of ionic solution is constant. So in this work and our previous work (Ma et al., 2018), we set the back-gate voltage as 20 V in DG mode where the maximum transconductance value is located in order to achieve the best biosensor performance. Additionally, the applied back-gate bias may lead to enhancement of the signal to noise ratio (SNR) of NR-ISFET, and hence, the sensitivity is higher with lower LOD (Zadorozhnyi and Vitusevich, 2016).

Moreover, in order to further investigate the effect of back gate of NR-ISFET device on biosensor performance, concentration-dependent PSA detection in 100 mM PB was conducted with different back-gate voltages. The sensor response curves of V_{BG} = 5 V, 10 V, 15 V and 25 V are illustrated in Fig. 4(a)–(d), respectively. When the V_{BG} was increased from 5 V to 25 V, the absolute conductance values increased, and conductance variation was also enhanced with reduced LOD. It reveals that the sensor performance can be improved with increased back-gate bias. The calibration curves can be plotted based on fitting by the Langmuir model for different bias conditions as shown in Fig. 4(e) with replotted log-scale curves in the insets. The equilibrium constants (k = ~10^8 M^{-1}) calculated according to Equation (1) in four bias conditions agree well with the previously reported results of protein adsorption (Latour, 2015; Tarasov et al., 2015). The influence of back-gate bias on sensor performance was summarized in Fig. 4(f), in which the conductance variation as a function of back-gate voltages for different PSA concentrations were plotted. The conductance variation increased gradually when V_{BG} increased from 0 V to 20 V, and became almost saturated after V_{BG} further increased to 25 V. The LOD reduced from 1 nM to 100 pM when V_{BG} increased from 0 V to 5 V, and further reduced to 10 pM when V_{BG} increased to 10–25 V. It is clearly shown that the applied back-gate bias enabled the enhancement of sensor performance when V_{BG} increased from 0 V to 20 V, and it became almost stable when V_{BG} further increased to 25 V. Therefore, it also proves that the best biosensor performance is achieved when the back-gate voltage is 20 V where the maximum transconductance value is reached. And V_{BG} = 20 V is considered as the optimized back-gate bias condition for our NR-ISFET biosensor. The results above clearly indicate the significance of the back gate on the performance improvement of NR-ISFET biosensor.

3.3 PSA detection in human plasma

To demonstrate the potential of our NR-ISFET biosensor for clinical applications, PSA detection in human plasma was conducted by the NR-ISFET biosensor system in both SG and DG modes. It was more relevant and significant to achieve direct detection in human plasma samples as compared to simple ionic solutions. The human plasma samples were used without further purification and directly spiked with PSA of different concentrations. In SG mode, the conductance as a function of time with the delivery of PSA of 1 nM to 1 μM in human plasma at t = 180 s, followed by switching to plasma at t = 900 s is shown in Fig. 5(a). The calibration curve derived from the fitting method mentioned above indicates the equilibrium constant of $k = 1.32\times10^7$ M^{-1} with excellent fitting (R^2 = 0.9899) for the protein adsorption process with a linear detection region from 10 nM to 1 μM of PSA (Fig. 5(b)). With the back-gate bias V_{BG} = 20 V, the real-time response curves of

concentration-dependent PSA detection in human plasma was illustrated in Fig. 5(c), in which the Langmuir adsorption isotherm can be well applied to the data (R^2 = 0.9600) with the equilibrium constant of $k = 8.43\times10^7$ M^{-1}. The results demonstrate that PSA of 100 pM to 1 μM in human plasma can be directly detected with a linear detection range of 1 nM to 100 nM (Fig. 5(d)). Furthermore, the LOD of 100 pM PSA can meet the clinical requirements assuming a measured PSA concentration of <120 pM in human body as clinically safe (Yu et al., 2004). The significance of adding back gate in the sensing measurements on the performance of NR-ISFET biosensor was also demonstrated.

As shown in Table 1, the performance of several ISFET-based PSA detection methods in high ionic solutions and human plasma are summarized and compared. Our NR-ISFET biosensor enables specific PSA detection based on antibody-antigen binding in broader detection range with lower LOD, and it can be used for direct real-time detection of PSA in human plasma samples which shows great potential for clinical applications as compared to the previously reported results. Furthermore, the use of back gate bias can further improve the sensing performance of NR-ISFET biosensor in terms of detection range and LOD.

Conclusions

In this paper, real-time detection of PSA in high ionic strength solution and human plasma is demonstrated by using a dual-gate PEG-modified NR-ISFET biosensor system in both SG and DG modes, which has overcome the limitation of Debye screening effect. Direct and selective detection based on antibody-antigen binding of PSA of 10 pM to 1 μM with linear detection region from 100 pM to 100 nM was achieved by the NR-ISFET biosensor in DG mode without prior desalting. Furthermore, the effect of different back-gate biases of NR-ISFET on the biosensor performance was investigated. More significantly, real-time specific detection of PSA of 100 pM to 1 μM in human plasma by the NR-ISFET biosensor in DG mode was successfully demonstrated, which can meet the clinical requirements assuming a measured PSA concentration of <120 pM in human body as clinically safe. The concept of using the dual-gate NR-ISFET biosensor for direct quantification of biomarker proteins in human blood provides a simple yet high performance method for low-cost clinical applications. Moreover, it is possible to achieve the multiplex detection of various cancer biomarkers by the NR-ISFET biosensor system because single NR-ISFET chip can be integrated with multiple microchannels to conduct different functionalization simultaneously as well as the synchronous testing of several NR-ISFETs.

Acknowledgements

This work was financially supported by grants from the National Natural Science Foundation of China (No. 91123018, 51625504, 61671368), Shaanxi Natural Science Foundation (2014JM7277), and Science and Technology Planning Project of Guangdong Province, China (2017A010103004).

The authors would like to thank technical staff at the State Key Laboratory for Manufacturing System Engineering in Xi'an Jiaotong University for device fabrication support and the Xi'an Central Hospital for providing human plasma samples.

References

Ambrosi, A., Airo, F., Merkoci, A., 2010. Anal. Chem. 82(3), 1151-1156.

Bergveld, P., 1972. IEEE Trans. Biomed. Eng. 5, 342-351.

Bergveld, P., 2003. Sens. Actuators. B Chem. 88(1), 1-20.

Bunimovich, Y.L., Shin, Y.S., Yeo, W., Amori, M., Kwong, G., Heath, J.R., 2006. J. Am. Chem. Soc. 128(50), 16323-16331.

Chen, S., Bomer, J.G., Carlen, E.T., van den Berg, A., 2011. Nano Lett. 11(6), 2334-2341.

Duan, X., Li, Y., Rajan, N.K., Routenberg, D.A., Modis, Y., Reed, M.A., 2012. Nat. Nanotechnol. 7(6), 401-407.

Elfström, N., Karlström, A.E., Linnros, J., 2008. Nano Lett. 8(3), 945-949.

Elnathan, R., Kwiat, M., Pevzner, A., Engel, Y., Burstein, L., Khatchtourints, A., Lichtenstein, A., Kantaev, R., Patolsky, F., 2012. Nano Lett. 12(10), 5245-5254.

Esashi, M., 1975. J. Jpn. Soc. Appl. Phys. 44, 339-343.

Gao, A., Lu, N., Wang, Y., Dai, P., Li, T., Gao, X., Wang, Y., Fan, C., 2012. Nano Lett. 12(10), 5262-5268.

Gao, N., Gao, T., Yang, X., Dai, X., Zhou, W., Zhang, A., Lieber, C.M., 2016. Proc. Natl. Acad. Sci. U.S.A. 113(51), 14633-14638.

Gao, N., Zhou, W., Jiang, X., Hong, G., Fu, T., Lieber, C.M., 2015. Nano Lett. 15(3), 2143-2148.

Hakim, M.M., Lombardini, M., Sun, K., Giustiniano, F., Roach, P.L., Davies, D.E., Howarth, P.H., de Planque, M.R., Morgan, H., Ashburn, P., 2012. Nano Lett. 12(4), 1868-1872.

Hao, Y., Zhou, B., Wang, F., Li, J., Deng, L., Liu, Y., 2014. Biosens. Bioelectron. 52, 422-426.

Hayes, J.H., Barry, M.J., 2014. JAMA. 311(11), 1143−1149.

Hu, C., Zeimpekis, I., Sun, K., Anderson, S., Ashburn, P., Morgan, H., 2016. Anal. Chem. 88(9), 4872-4878.

Jang, H., Cho, W., 2011. Appl. Phys. Lett. 99(4), 043703.

Knopfmacher, O., Tarasov, A., Fu, W., Wipf, M., Niesen, B., Calame, M., Schonenberger, C., 2010. Nano Lett. 10(6), 2268-2274.

Kumar M, A., Jung, S., Ji, T., 2011. Sensors. 11(5), 5087-5111.

Latour, R.A., 2015. J. Biomed. Mater. Res. A. 103(3), 949-958.

Levine, I.N., 2009. Physical Chemistry, sixth ed. McGraw-Hill, Boston.

Ma, S., Lee, Y.-K., Zhang, A.P., Li, X., 2018. Sens. Actuators. B Chem. 264, 344-352.

Maehashi, K., Katsura, T., Kerman, K., Takamura, Y., Matsumoto, K., Tamiya, E., 2007. Anal. Chem. 79(2), 782-787.

Matsuo, T., Esashi, M., 1981. Sens. Actuators. 1, 77-96.

Nair, P.R., Alam, M.A., 2008. Nano Lett. 8(5), 1281-1285.

Patolsky, F., Zheng, G., Lieber, C.M., 2006. Nat. Protoc. 1(4), 1711-1724.

Peretz-Soroka, H., Pevzner, A., Davidi, G., Naddaka, V., Tirosh, R., Flaxer, E., Patolsky, F., 2013. Nano Lett. 13(7), 3157-3168.

Pud, S., Li, J., Sibiliev, V., Petrychuk, M., Kovalenko, V., Offenhausser, A., Vitusevich, S., 2014. Nano Lett, 14(2), 578-584.

Selvanayagam, Z.E., Neuzil, P., Gopalakrishnakone, P., Sridhar, U., Singh, M., Ho, L., 2002. Biosens. Bioelectron. 17(9), 821-826.

Shalev, G., Cohen, A., Doron, A., Machauf, A., Horesh, M., Virobnik, U., Ullien, D., Levy, I., 2009. Sensors. 9(6), 4366-4379.

Shalev, G., Rosenwaks, Y., Levy, I., 2012. Biosens. Bioelectron. 31(1), 510-515.

Stern, E., Klemic, J.F., Routenberg, D.A., Wyrembak, P.N., Turner-Evans, D.B., Hamilton, A.D., LaVan, D.A., Fahmy, T.M., Reed, M.A., 2007. Nature. 445, 519.

Stern, E., Vacic, A., Rajan, N.K., Criscione, J.M., Park, J., Ilic, B.R., Mooney, D.J., Reed, M.A., Fahmy, T.M., 2010. Nat. Nanotechnol. 5(2), 138-142.

Stern, E., Wagner, R., Sigworth, F.J., Breaker, R., Fahmy, T.M., Reed, M.A., 2007. Nano Lett. 7(11), 3405-3409.

Sun, K., Zeimpekis, I., Hu, C., Ditshego, N.M., Thomas, O., de Planque, M., Chong, H., Morgan, H., Ashburn, P., 2016. Nanotechnology. 27(28), 285501.

Tarasov, A., Fu, W., Knopfmacher, O., Brunner, J., Calame, M., Schönenberger, C., 2011. Appl. Phys. Lett. 98(1), 012114.

Tarasov, A., Tsai, M., Flynn, E.M., Joiner, C.A., Taylor, R.C., Vogel, E.M., 2015. 2D Mater. 2(4), 044008.

Toumazou, C., Thay, T.S., Georgiou, P., 2014. Philos. Trans. A. Math. Phys. Eng. Sci. 372(2012), 20130112.

Xie, P., Xiong, Q., Fang, Y., Qing, Q., Lieber, C.M., 2012. Nat. Nanotechnol. 7(2), 119-125.

Xu, S., Liu, Y., Wang, T., Li, J., 2011. Anal. Chem. 83(10), 3817-3823.

Yacoub-George, E., Wolf, H., Koch, S., Woias, P., 1996. Sens. Actuators. B Chem. 34(1-3), 429-434.

Yu, F., Persson, B., Löfås, S., Knoll, W., 2004. Anal. Chem. 76(22), 6765-6770.

Yu, R., Pan, C., Wang, Z.L., 2013. Energy Environ. Sci. 6(2), 494-499.

Zadorozhnyi, I., Vitusevich, S., 2016. Solid-State Device Research Conference (ESSDERC), 2016 46th European. IEEE. 393-396.

Zeimpekis, I., Sun, K., Hu, C., Ditshego, N., Thomas, O., de Planque, M.R., Chong, H.M., Morgan, H., Ashburn, P., 2016. Nanotechnology. 27(16), 165502.

Zeng, S., Baillargeat, D., Ho, H.P., Yong, K.T., 2014. Chem. Soc. Rev. 43(10), 3426-3452.

Zhang, G., Zhang, G., Chua, J.H., Chee, R., Wong, E.H., Agarwal, A., Buddharaju, K.D., Singh, N., Gao, Z., Balasubramanian, N., 2008. Nano Lett. 8(4), 1066-1070.

Zheng, G., Patolsky, F., Cui, Y., Wang, W.U., Lieber, C.M., 2005. Nat. Biotechnol. 23(10), 1294-1301.

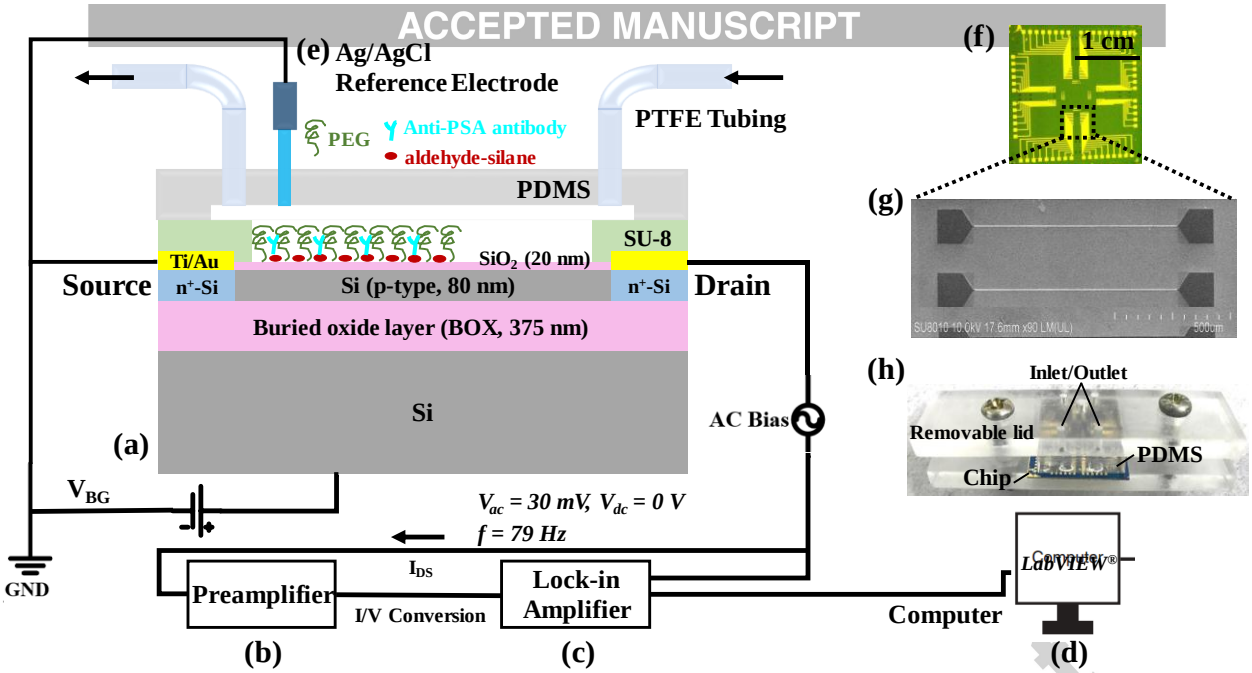

Fig 1: NR-ISFET biosensor system for protein detection: (a) Schematic of the NR-ISFET device with surface modification of aldehyde-silane (red), PEG (green) and anti-PSA antibody receptors (aqua) on the top oxide layer and PDMS-based microchannel for sample delivery by PTFE tubing, (b) lock-in amplifier, (c) current preamplifier, (d) data acquisition, and (e) Ag/AgCl reference electrode used for conductance measurement, (f) photograph of the NR-ISFET chip, (g) SEM image of the NR-ISFETs and (h) photograph of the packaged NR-ISFET chip with PDMS-based microchannels.

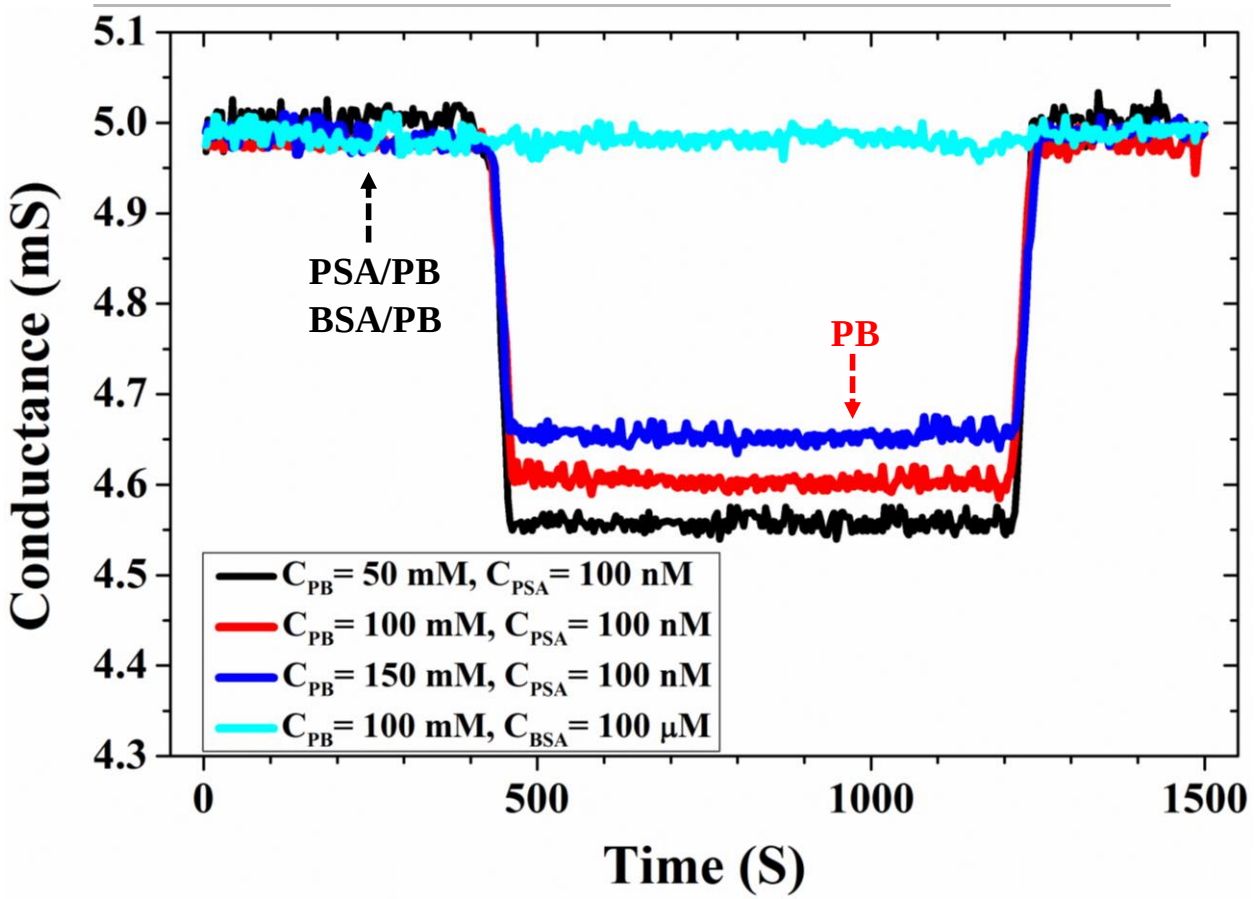

Fig 2: Real-time conductance measurements of the NR-ISFET (W = 5 µm) with surface modification after delivery of PSA (100 nM) in PB solutions with different ionic strengths (50 mM, 100 mM and 150 mM) and BSA (100 µM) in PB solution (100 mM), followed by switching to pure PB solutions. The black and red dashed arrows indicate the delivery of protein (t = 250 s) and buffer solutions (t = 960 s), respectively.

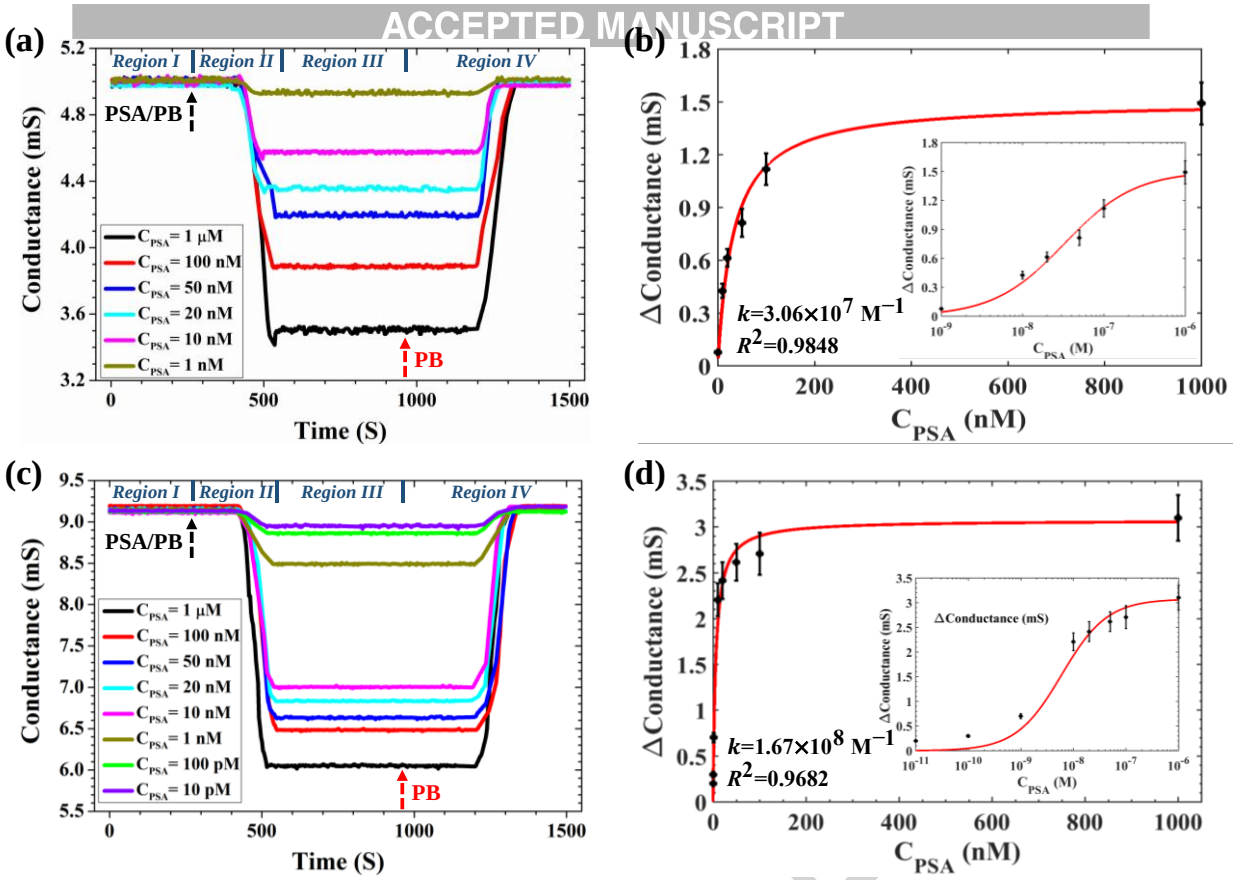

Fig 3: Real-time conductance measurements of the NR-ISFET (W = 5 μm) with surface modification in high ionic strength solution (100 mM) after delivery of (a) PSA with different concentrations ranging from 1 nM to 1 μM in SG mode (V_{BG} = 0 V) and (c) from 10 pM to 1 μM in DG mode (V_{BG} = 20 V). The black and red dashed arrows indicate the delivery of protein (t = 250 s) and buffer solutions (t = 960 s), respectively. The plot of conductance variation as a function of PSA concentrations and corresponding fitting curves based on Langmuir adsorption isotherm (b) in SG mode with $k = 3.06\times10^{7}$ M^{-1} and (d) DG mode with $k = 1.67\times10^{8}$ M^{-1} (the logarithmic curves are shown in insets).

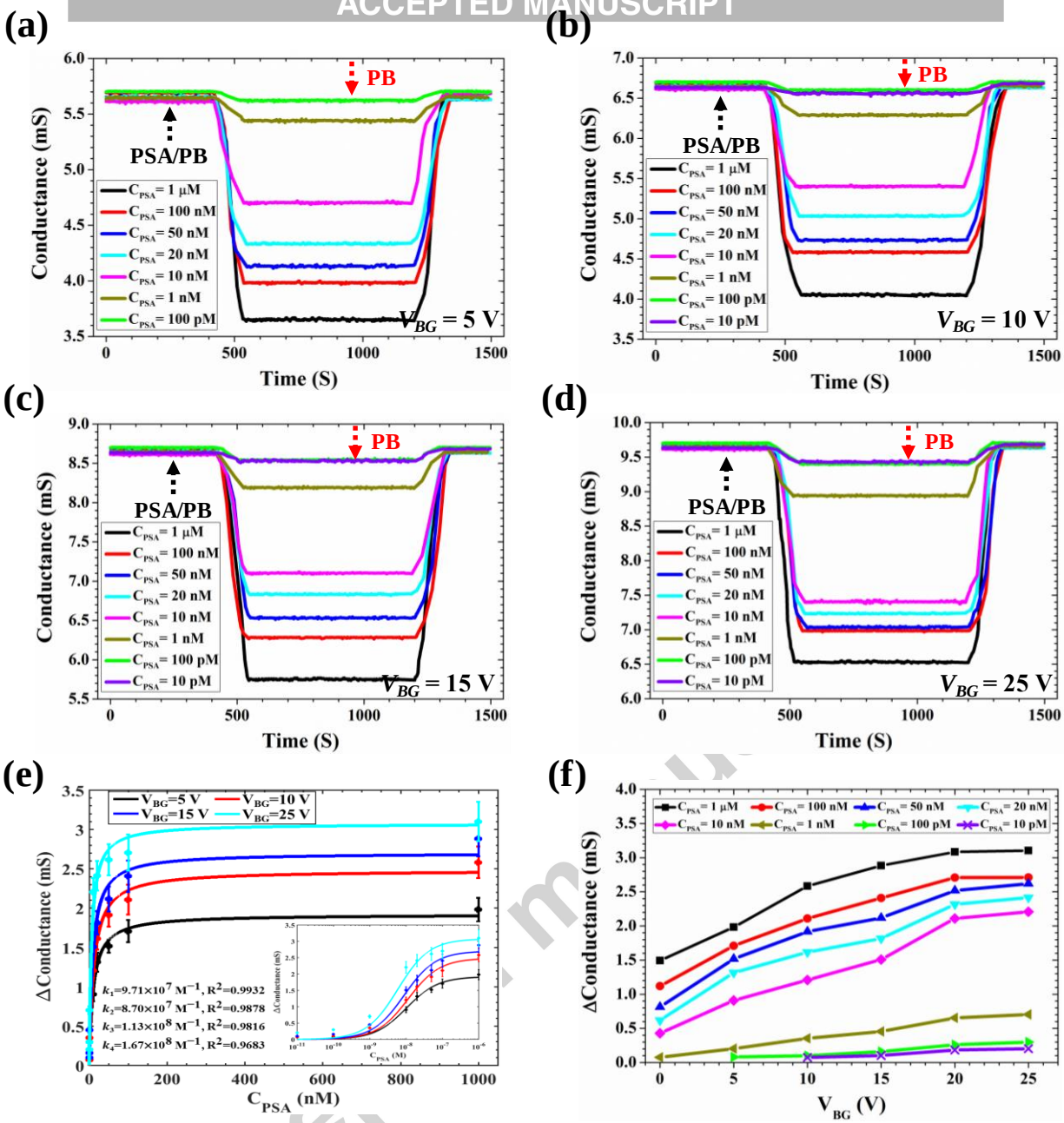

Fig 4: (a)–(d) Real-time conductance measurements of the NR-ISFET (W = 5 μm) with surface modification in high ionic strength solution (100 mM) after delivery of PSA solutions at different back-gate biases (V_{BG} = 5, 10, 15, 25 V). The black and red dashed arrows indicate the delivery of protein (t = 250 s) and buffer solutions (t = 960 s), respectively. (e) The plot of conductance variation as a function of PSA concentrations and corresponding fitting curves based on Langmuir adsorption isotherm for different back-gate biases (the inset shows the logarithmic curves). The equilibrium constants k of them are calculated as shown in the figure. (f) The plot of conductance variation as a function of back-gate voltages for different PSA concentrations.

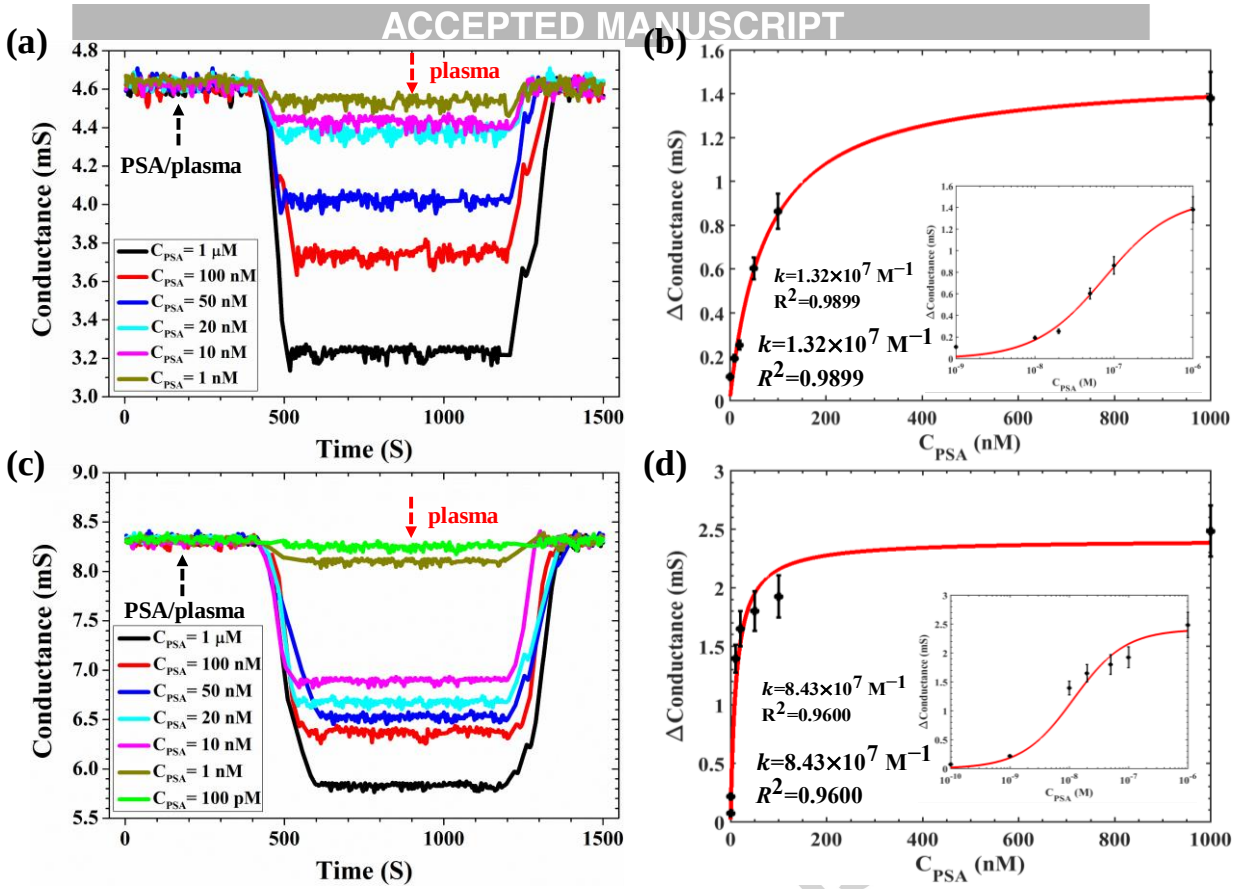

Fig 5: Real-time conductance measurements of the NR-ISFET (W = 5 μm) with surface modification in human plasma samples spiked with PSA of different concentrations ranging from 1 nM to 1 μM in SG mode (V_{BG} = 0 V) and (c) from 100 pM to 1 μM in DG mode (V_{BG} = 20 V). The black and red dashed arrows indicate the delivery of plasma spiked with PSA (t = 180 s) and plasma (t = 900 s), respectively. The plot of conductance variation as a function of PSA concentrations and corresponding fitting curves based on Langmuir adsorption isotherm (b) in SG mode with $k = 1.32\times10^7$ $M^{-1}$and (d) DG mode with $k = 8.43\times10^7$ M^{-1} (the logarithmic curves are shown in insets).

Table 1: Performance comparison of ISFET-based PSA detection in high ionic solution and human plasma

		Detection principle	*Detection condition*	*Detection range*	*Equilibrium constant*
Si NW-ISFET [34]		Nonspecific binding	100 mM PB	10 nM~1 μM	6.40×10^6 M^{-1}
Graphene-based ISFET [35]		Nonspecific binding	100 mM PB	1 nM~1 μM	7.90×10^6 M^{-1}
Si NR-ISFET (this paper)	**SG mode**	**Specific binding**	**100 mM PB**	**1 nM~1 μM**	**3.06×10^7 M^{-1}**
			Human plasma	**1 nM~1 μM**	**1.32×10^7 M^{-1}**
	DG mode (V_{BG} = 20 V)	**Specific binding**	**100 mM PB**	**10 pM~1 μM**	**1.67×10^8 M^{-1}**
			Human plasma	**100 pM~1 μM**	**8.43×10^7 M^{-1}**

Highlights

- A dual-gate nanoribbon-based ion-sensitive field-effect Transistor (NR-ISFET) biosensor for direct label-free protein detection in high ionic strength solution and human plasma is demonstrated, which has overcome the limitation of Debye screening effect.
- Compared with previously reported results, the NR-ISFET biosensor in dual-gate (DG) mode enables selective prostate specific antigen (PSA) detection in 100 mM phosphate buffer (PB) based on antibody-antigen binding in broader detection range (10 pM to 1 μM) with lower LOD (10 pM).
- The effect of different back-gate biases (V_{BG}) of NR-ISFET on the biosensor performance has been investigated, and the optimized back-gate bias for best biosensor performance has been obtained. The applied back-gate bias and utilization of lock-in amplifier for conductance measurements are beneficial to the signal-to-noise ratio (SNR) enhancement resulting in higher sensitivity for protein detection.
- Direct PSA detection of 100 pM to 1 μM in human plasma using PEG-modified NR-ISFET in DG mode is demonstrated which can meet the clinical requirements.